Optoelectronic Signatures of DNA-Based Hybrid Nanostructures

Milana Vasudev, Tsai-Chin Wu, Sushmita Biswas, Mitra Dutta, *Fellow, IEEE*, Michael A. Stroscio, *Fellow, IEEE*, Stan Guthrie, Mark Reed, *Fellow, IEEE*, Kellie P. Burris, and C. Neal Stewart, Jr.

***Abstract*—This paper presents a characterization of the vibrational modes of nanostructure–DNA complexes immobilized on substrates, such as silver-coated microspheres and silver nanostructure array DNA strands end terminated with titanium dioxide (TiO_2) nanoparticles are used to study UV-induced cleaving of DNA molecules functionalized with indirect-bandgap semiconductors. In addition, conventional DNA-based molecular beacons were designed and applied in the detection of DNA of selected organisms. Micro-Raman (μRaman) measurements of DNA in water have proven to be a major challenge because of: 1) weak DNA signatures in solution; 2) changes in structural conformations of the DNA; and 3) environmental effects, such as temperature and pH of the solution in which DNA is suspended. We have studied optoelectronic properties of nanostructure–DNA complexes immobilized on silver nanosphere substrates as well as on Ag-coated micro- and nanostructures. In this research, self-assembled monolayers of DNA formed on these substrates were studied using μRaman techniques. These Raman spectra were used to identify prominent vibrational modes of DNA, and to characterize DNA Raman spectra for both B-DNA with a right-handed double helix, and Z-DNA with a left-handed double helix (S. C. Ha, K. Lowenhaupt, A. Rich, Y. Kim, and K. Kim, "Crystal structure of a junction between B-DNA and Z-DNA reveals two extruded bases," Nature, Vol. 437, pp. 1183–1186, 2005). These Raman-based studies of the conformational states of DNA employ pH-changing trivalent salts, methylation of cytosine bases, and alternating GC bases. Moreover, DNA strands terminated with titanium dioxide (TiO_2) nanoparticles were observed to undergo cleaving upon UV illumination.**

***Index Terms*—DNA, micro-Raman (μRaman), molecular beacon (MB), molecular conformation, quantum dots.**

Manuscript received November 30, 2009; accepted June 29, 2010. Date of publication August 5, 2010; date of current version January 26, 2011. This work was supported in part by the U.S. ARO-DTRA under Grant W911NF-08–1-0114. The review of this paper was arranged by Associate Editor P. J. Burke.

M. Vasudev and T.-C. Wu are with the Department of Bioengineering, University of Illinois, Chicago, IL 60607 USA (e-mail: mvasud2@uic.edu; twu22@uic.edu).

S. Biswas is with the Department of Electrical and Computer engineering, University of Illinois, Chicago, IL 60607 USA (e-mail: sbiswa2@ece.uic.edu).

M. Dutta is with the Department of Electrical and Computer engineering, and Physics, University of Illinois, Chicago, IL 60607 USA (e-mail: dutta@uic.edu).

M. A. Stroscio is with the Departments of Bioengineering, Electrical and Computer Engineering, and Physics, University of Illinois, Chicago, IL 60607 USA (e-mail: stroscio@uic.edu).

S. Guthrie and M. Reed are with the School of Engineering and Applied Sciences, Yale University New Haven, CT 06510 USA (e-mail: stan.guthrie@yale.edu; mark.reed@yale.edu).

K. P. Burris is with the Departments of Plant Sciences, and Food Science & Technology, University of Tennessee, Knoxville, TN 38237 USA (e-mail: kparks2@utk.edu).

C. N. Stewart Jr. is with the Department of Plant Sciences at University of Tennessee, Knoxville, TN 38237 USA (e-mail: nealstewart@utk.edu).

Color versions of one or more of the figures in this paper are available online at http://ieeexplore.ieee.org.

Digital Object Identifier 10.1109/TNANO.2010.2064174

I. Introduction

THE USE of self-assembled DNA monolayers on polymeric nanosphere substrates with silver deposition is undertaken to assess the role of layered structures on the vibrational modes of DNA. The advantage of using metallic substrates is the amplification of the Raman signatures at close distances from their surface due to the localized surface plasmons. Surface-enhanced Raman spectroscopy (SERS) shows great promise in overcoming the low-sensitivity problems inherent in Raman spectroscopy by allowing the detection of a broad range of molecules. This method incorporates the analytical advantages of Raman spectroscopy with the additional possibility of detecting very low concentration of the biological samples. The enhancement mechanisms can be attributed to the electromagnetic field. SERS has demonstrated an ability to detect single molecules including the single DNA bases, which makes it a good method for biomolecular detection as well as being a label-free method. Nanoparticles dimers are known to produce larger SERS enhancement, which are known as "*hot spots*" when separated by nanometer-scale gaps. Therefore, nanoparticles of size 500 nm also produce huge SERS enhancement due to the presence of these hot spots. Some of the substrates used in these experiments have an average size of 500 nm, which can lead to the enhancement of the Raman signatures. The characterization of two such substrates is presented here. E-beam deposition of silver on microsphere substrates [1] as well as the e-beam lithography on silicon dioxide substrates [2] has been used for the synthesis of the two different substrates for the immobilization of DNA.

DNA-based sensors are important diagnostic tools in medical analysis, pharmacology, as well as in the food industry. One of the most sought after forms of detection is the detection of single nucleotide polymorphisms (SNP), which is a genetic variation involving the change in a single nucleotide. Molecular beacons (MBs) are single strands of DNA, which could be used as hybridization probes that can potentially detect SNPs [3]. In this paper, two such beacons will be highlighted one of which can be used for the use in cancer detection (*BRCA1* gene) as well as a beacon for the detection of food-borne pathogen (*Salmonella serotype typhimurium*).

II. Procedure

Arrays of silver-coated close-packed polystyrene beads were prepared as the substrate for self-assembled DNA layers used in this study of DNA. These substrates are fabricated on 18-mm-diameter glass cover slips (No. 2, Fisher Scientific).

These substrates were cleaned using the Piranha solution ($1:330\%H_2O_2:H_2SO_4$) at 80 °C for 30 min, and rendered hydrophilic by using 5:1:1 ($H_2O:NH_4OH:30\%H_2O_2$) with sonication for 1 h. Latex polystyrene spheres with diameters of 390 nm were dispersed on the cleaned slides by drop coating as well as spin coating 5–10 μL of these white carboxyl substituted polystyrene latex nanospheres (Duke Scientific). Silver is then thermally deposited on the nanosphere mask using the Varian e-beam deposition system with thickness varying from 100 to 200 nm at deposition rate of 1 Å/s at 10^{-7} torr pressure [1]. The B–Z transitions of the DNA were studied on the silver nanosphere substrates, which were deposited on a glass surface.

A. B–Z Transitions on Silver Nanosphere Substrates

In this study of B–Z transitions in DNA and related Raman spectra, DNA-based self-assembled monolayers (SAMs) of DNA were fabricated in order to ensure a high density of DNA molecules is sampled in the Raman scattering process. DNA in nature can exist in A-, B-, and Z-forms as its native form. The most commonly known conformation is the B-form, which is a right-handed double helix, whereas the Z-form is a left-handed double helix [4].

DNA can switch from one conformation to the other when there are controlled conditions including the changes in concentrations of trivalent salts, such as hexamine cobalt chloride, and having an alternating stretch of purine and pyrimidine bases in the DNA structure. It has been previously investigated that the addition of salts, such as hexamine cobalt chloride, can cause the DNA to switch from the B-form to the Z-form, and this only occurs in series of cytosine–guanine (C-G) dinucleotide base repeats. The DNA then changes from a right-handed helix to a left-handed one and the change in the twist is estimated to be 128° for each dinucleotide (CG) [5].

For these B–Z transition studies, the DNA strand immobilized on the Ag nanosphere-based substrate was 5′-GAG CGG CTT/**iMe-dC**/G/**iMe-dC**/GCG CG/**iMe-dC**/G/**iMe-dC**/ G CGC GCG CAG/*3ThioMC3-D*/; where, iMe-dC is the methylated cytosine base, which is known to promote B–Z transitions, and */3ThioMC3-D/* is the 3′ thiol modification required for the immobilization on the modified silver nanosphere-based substrate [6], [7]. The presence of the alternating CG bases also is a known factor in the B–Z transitions of DNA. For B-DNA, the conditions are as follows: 10 mM of NaCl in potassium phosphate buffer (pH 6.7). The transition of the B-DNA to the Z-form is facilitated in solution due to the presence of the trivalent salt, cobalt hexamine chloride. For Z-DNA, the conditions are modified from those specified for B-DNA by adding 5 mM of $MgCl_2$, 100 mM of NaCl, and 200 μM of $CO(NH_3)_6Cl$ in sodium cacodylate buffer (pH 6.7) [8]. The transition of B-DNA to Z-DNA is done in solution before being immobilized on the silver nanosphere substrates. To form mixed DNA/mercapto hexanol monolayers, the previously described DNA-functionalized substrates were immersed in a 1-mM aqueous solution of mercapto hexanol (MCH), Sigma for 5 min and rinsed thoroughly.

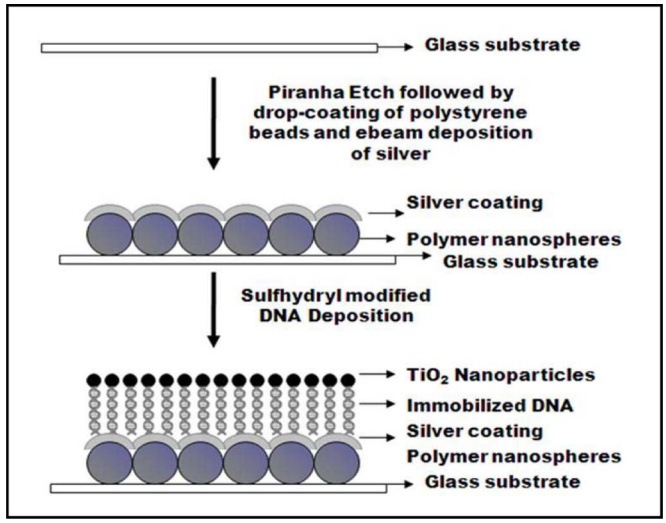

Fig. 1. Illustration of the titanium dioxide nanoparticles attached to DNA immobilized on silver-coated nanosphere substrates.

Mercapto hexanol is used as a spacer in self-assembled monolayers of DNA because it prevents the nonspecific adhesion of DNA to the substrate by preventing the DNA backbone from coming in contact with the silver substrate [9]. It also prevents the DNA strands from clustering together. Complementary DNA strands are added making double stranded DNA on silver. A mixed monolayer of DNA and MCH is formed, since the thiol group on the MCH chemically adsorbs to the silver surface.

Raman spectra of the B-DNA and Z-DNA samples were acquired with a Renishaw micro-Raman (μRaman) apparatus with an Ar^+-ion laser (514.5 nm wavelength) at a power level of 8 mW. The Raman spectra were obtained with an 1800 gr/mm grating, providing a resolution of $0.8\,cm^{-1}$. The laser beam was focused on the sample through a specialized microscope lens objective (Olympus, 50×) down to a focal spot size of approximately 0.3 μm. The image of the substrate could be observed using a liquid-nitrogen-cooled charged-coupled device camera. The exact positioning of the substrate was accomplished using a translation stage. The scattered light was then analyzed with a UV double spectrometer. Fig. 2 presents the B-DNA spectra and Fig. 3 presents the Z-DNA spectra. Selected spectral lines from these μRaman studies of B-DNA and Z-DNA are summarized in Table I. These results indicate that selected Raman lines undergo shifts of several cm^{-1} as a result of the B–Z transition [10]–[12]. Otto *et al.*, had calculated the SERS peaks for each of the DNA bases, and the partial line assignments made in our SERS spectra are in accordance with this [10]. Consistent with other SERS investigations, by Otto *et al.*, of DNA, the B-form marker band at about $834\,cm^{-1}$ seen in conventional Raman spectra is absent; to our knowledge, the lack of this feature in experimental studies is not explainable by contemporary theoretical accounts of SERS spectra.

B. DNA Terminated with TiO_2 Nanoparticles

Previous studies of cleaving DNA, as reported in [13], have shown hole-based cleaving in TiO_2-DNA nanostructures

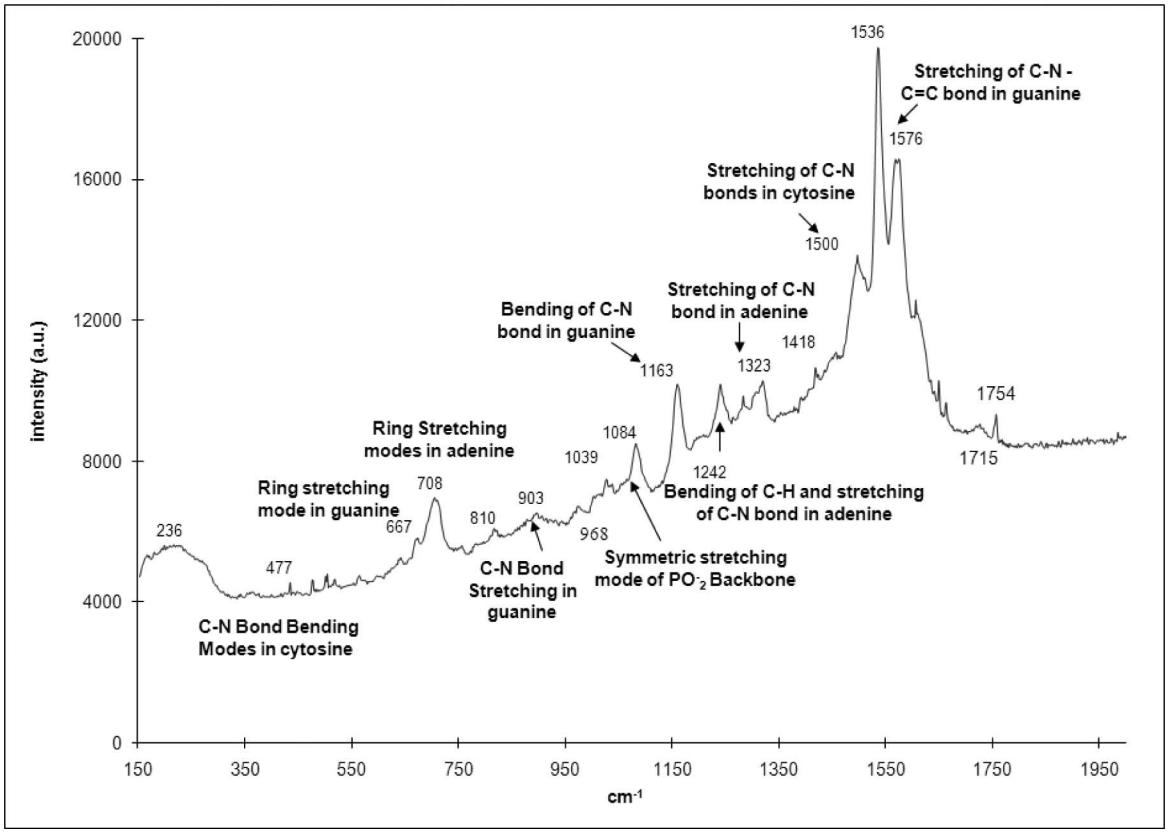

Fig. 2. Raman spectrum of DNA in B-form immobilized on the silver-modified substrate. Conditions: 8 mW power and 180 s.

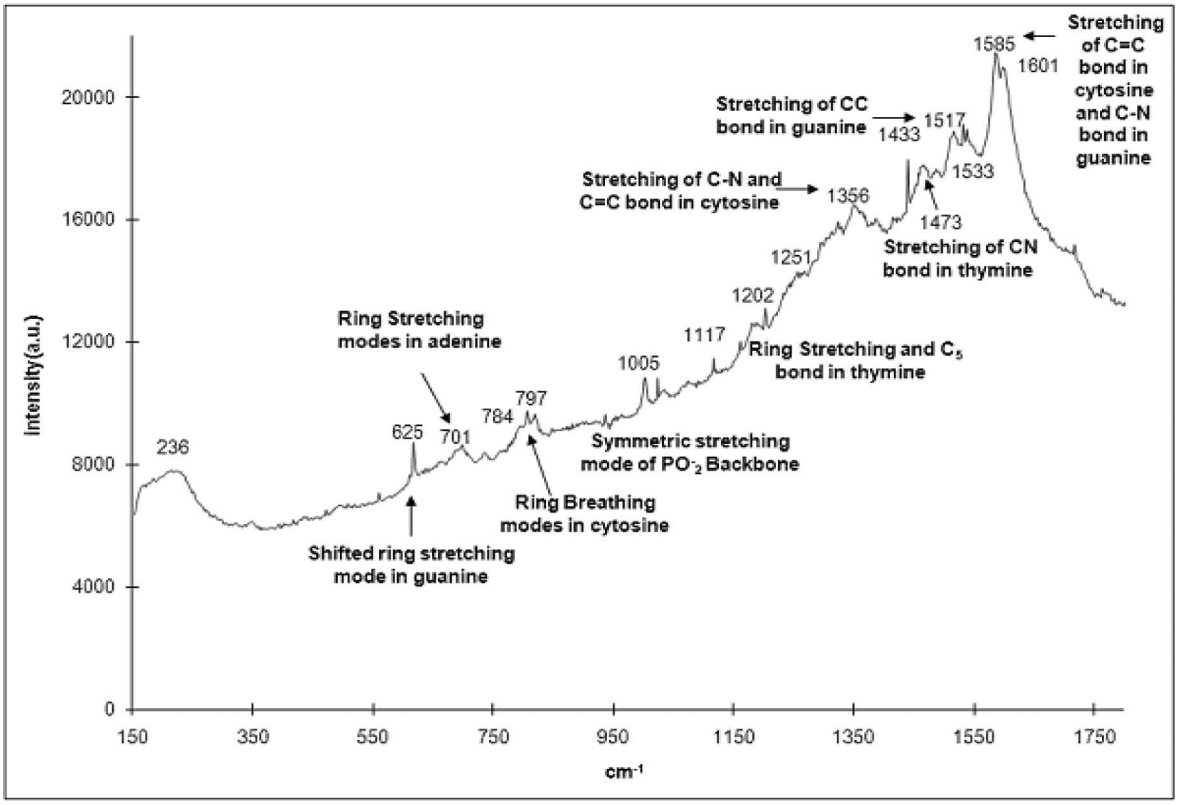

Fig. 3. Raman spectrum of DNA in Z-form immobilized on the silver-modified substrate. Conditions: 8 mW power and 180 s.

TABLE I
COMPARISON OF PEAKS IN B- AND Z-FORMS OF DNA ON SILVER NANOSPHERE SUBSTRATES

DNA Modes	B DNA	Z DNA
Ring stretching mode in guanine	667	625 (Shifted Peak)
Ring stretching mode in adenine	708	701
Ring breathing mode in cytosine	------	797
CN Bond stretching in guanine	903	------
Symmetric stretching of phosphate backbone	1084, 1039	1005
Backbone of the left-handed helix	------	789, 1433
Ring stretching and C_5 in thymine	------	1202
Bending of C-H and stretching of C-N bonds in adenine	1242	1251
Stretching of C-N bonds in adenine	1323	------
Stretching of C-N and C = C bond in cytosine	------	1356
Stretching of C-N bond in thymine	------	1473
Stretching of C-N bonds in cytosine	1500	------
Stretching of C=C bonds in guanine	------	1517
	1536	1533
Stretching of C-N – C=C bonds in guanine	1576	1585
Stretching of C = O bond in thymine	1715	------

performed under a variety of conditions. Herein, the first observation of this cleaving mechanism is reported for TiO_2-DNA complexes, where the DNA molecules form SAMs on a silver-coated nanosphere substrate (see Fig. 1). Since the guanine bases of the DNA have the lowest ionization potential among the four nucleotides, the presence of the three guanine bases creates a site of the very low ionization potential leading to the cleavage of the duplex DNA [14]. Charge separation in titanium dioxide nanoparticles via dopamine upon exposure to UV light has been studied and characterized previously [15], [16]. Excess of charges carriers, specifically holes created in titanium dioxide nanoparticles are then transferred into the DNA via dopamine due to the matching energy levels and the charges accumulate in the regions of low energy sites, such as G-rich sites, and cause cleaving of DNA.

The DNA strands used in these experiments for the charge transfer study via TiO_2 nanoparticles on the silver nanoparticle surface: 5′-/ThioMC6-D/ACT CGA GTA CAG CGA **CCC** AAC ATG AGA GAA C-3′, where the 5′ thiol is used for the immobilization on the silver surface and the complementary strand is attached to the TiO_2 nanoparticle on the 5′ end. The complementary strand is: 3′-TG AGC TCA TGT CGC T***GG G***TT GTA CTC TCT TG carboxy dT-5′, where the 5′ carboxy group is used for the attachment of TiO_2 nanoparticles. Using a procedure from Rajh *et al.* [15], [16], the carboxyl group on the 5′ end of the DNA is used for the attaching to the amine groups in the dopamine under inert gas (nitrogen) in the presence of chemicals, such as O-(N-succinimidyl) N, N, N', N' tetramethylammonium tetrafluoroborate (TSU) and N, N'-diisopropyl amine (i-PrEtN) in a solution of dimethyl formamide (DMF). The purification of the DNA-dopamine complex is performed via dialysis using DMF/water. Finally, TiO_2 nanoparticles are added in the presence of the glycidyl isopropyl ether, which allows the TiO_2 nanoparticles to attach to the DNA-dopamine complex. After exposure with UV radiation (326 nm) for 15 min, the substrates are washed to remove the DNA segments and the TiO_2 quantum dots that have been cleaved.

The sample is then analyzed via μRaman techniques, with the resulting spectrum for both cases being shown in Fig. 4, before exposure to UV light as shown, and Fig. 5, following the exposure to UV light, respectively. As is evident from Fig. 5, the Raman lines for the TiO_2 are absent indicating that the TiO_2 quantum dots are no longer anchored to the substrate via the DNA-linking molecules. This technique provides a very direct method of demonstrating the cleaving of DNA.

C. Silver Nanostructure Substrates by E-Beam Lithography

The self-assembly of DNA on a silver surface is accomplished using the procedure outlined in this section. A silicon substrate with a 200-nm-thick layer of SiO_2 is coated with 2.5 nm of Ti and 25 nm of Ag deposited via e-beam lithography. This substrate is patterned so that the Ag-coated regions form small arrays of Ag dots [2]. These arrays have dot sizes of 0.5 μm with dot pitches of 1, 2, and 5 μm. The overall field size is at least 10 μm $\times$ 10 μm. The DNA deposited on the Ag-coated dot regions is the *Bacillus subtillis* (BG) 168 simulant. Specifically, 20-base-long single-stranded oligonucleotides functionalized with disulfide groups on the 5′ end were reduced in the presence of tris(2-carboxyethyl) phosphine hydrochloride (TCEP·HCl) to form the thiol group on the 5′ end. DNA at a concentration of 1 to 5 μM and the TCEP·HCl (added in 100-fold excess) were allowed to react with the DNA at room temperature for 2 h.

Next, single-stranded DNA was adsorbed from 1- or 5-μM solutions in 1-M potassium phosphate buffer, pH 6.7, for 90 min. Finally, the slides are rinsed with Milli-Q water. The oligonucleotide structure selected was 5′-S-S-$(CH_2)_6$-AAG TAC TGC TTT CAG ACA TG-3′, with a thiol group at the 5′ end. As discussed previously by Globus *et al.*, the DNA strand is representative of the BG 168 (over 4M bases), since the ratios of Gs, Ts, As, and Cs are approximately those of BG 168 [17].

These surface-tethered HS-ssDNA oligonucleotides are hybridized to the complementary oligonucleotides (5′-NH_2-CA TGT CAG AAA GCA GTA CTT-3′). The hybridization process was performed in a 1.4-μM ssDNA-C solution in TE buffer at 37 °C for 90 min. The TE buffer was 10-mM 2-Amino-2-(hydroxymethyl)-1,3-propanediol, hydrochloride (tris-HCl), 1-mM ethylenediaminetetraacetic acid (EDTA), and 1-M NaCl at pH 7.0. Finally, samples were rinsed with TE buffer. In this study of the Raman spectra of SAMs, the planar substrates of previous studies [18] are replaced by an e-beam-fabricated patterned surface composed of an array of Ag-coated dots. The

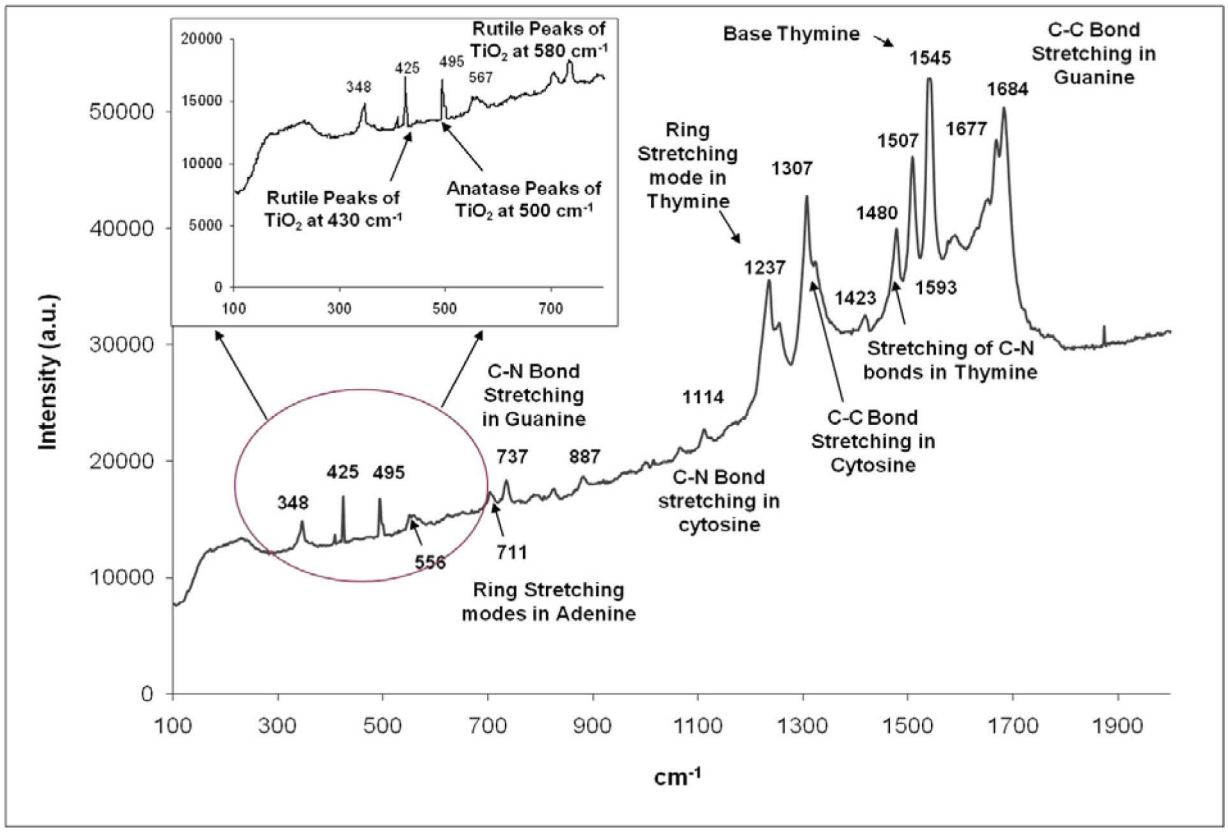

Fig. 4. Raman Spectra of the DNA on the silver nanosphere substrate end terminated with TiO_2 nanoparticles.

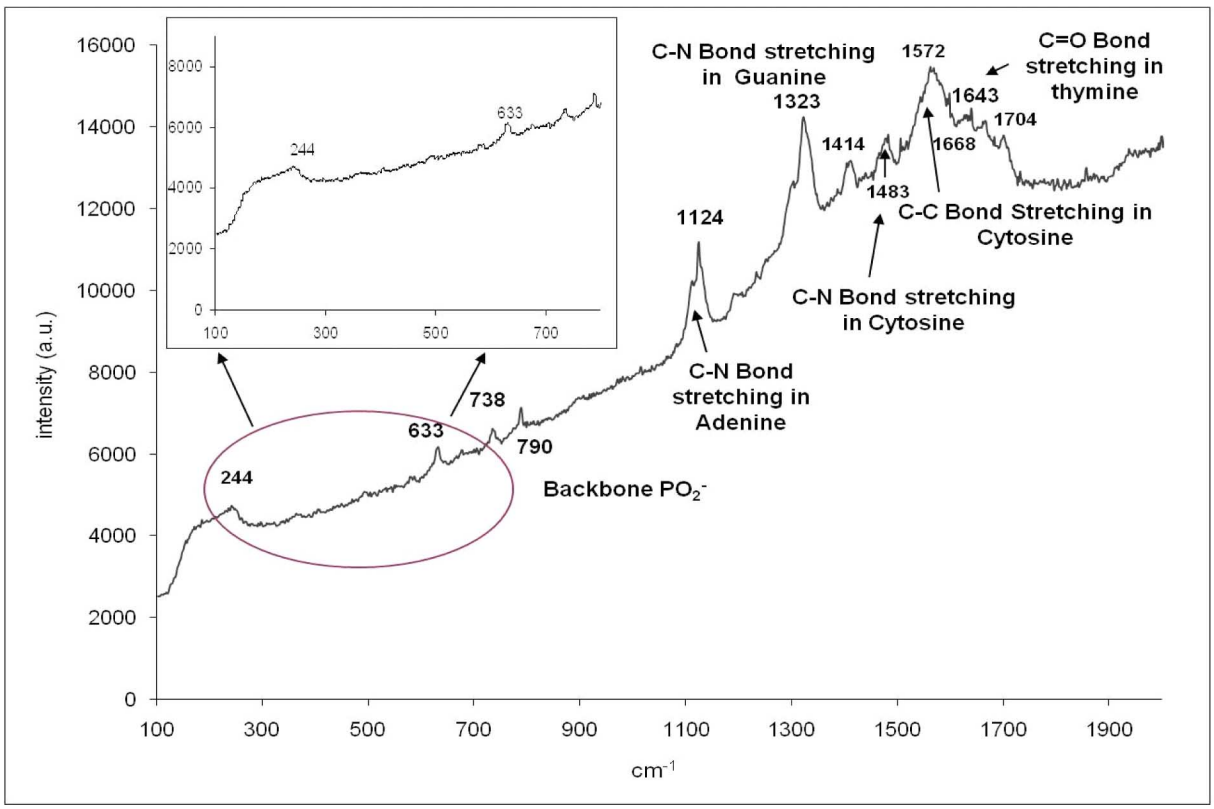

Fig. 5. Raman Spectra of the DNA on the silver nanosphere substrate after the TiO_2 nanoparticles are cleaved due to exposure to UV light.

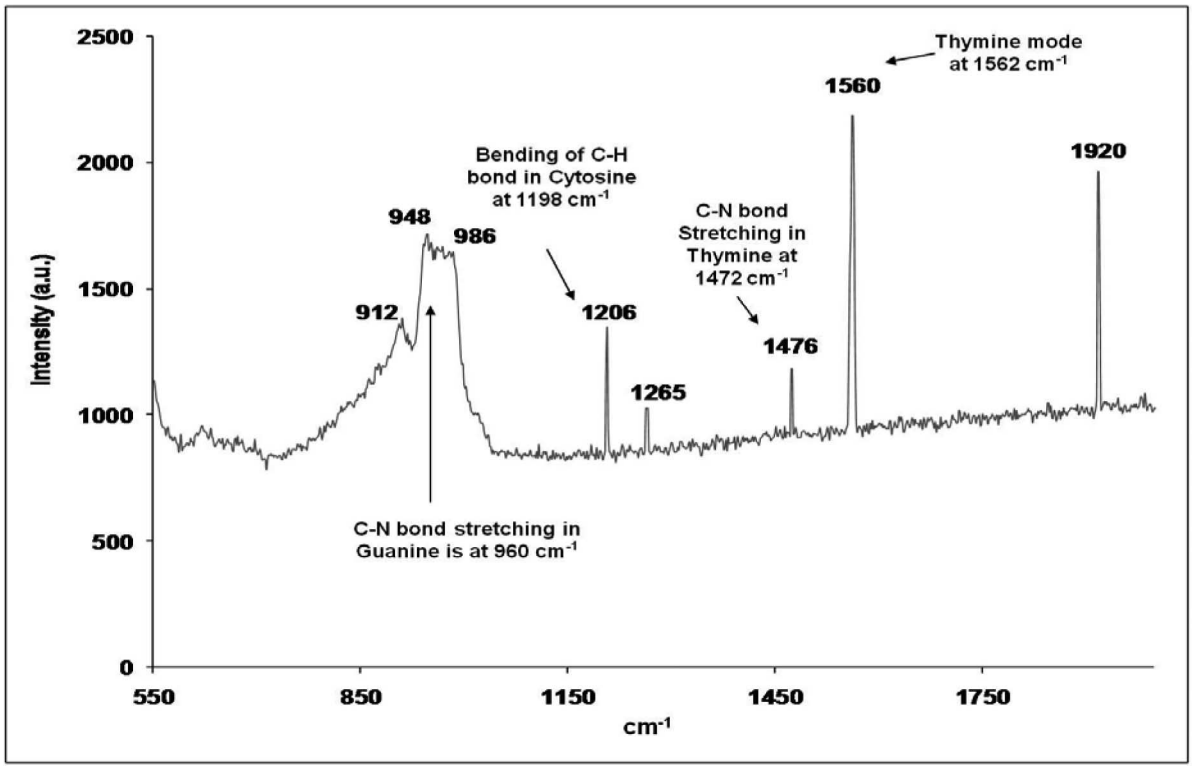

Fig. 6. Raman Spectra of the DNA on the silver nanostructured silver substrate by e-beam lithography. Conditions: 8 mW power, 120 s, and 5-μm pitch.

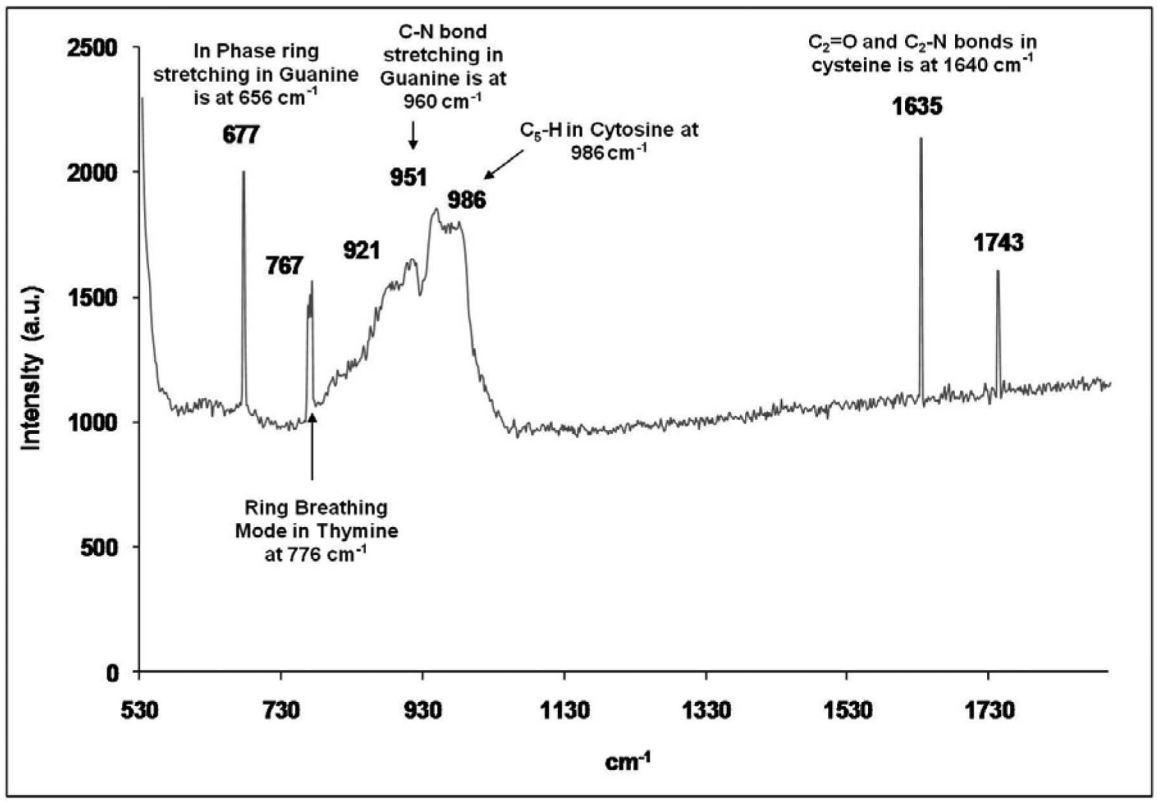

Fig. 7. Raman Spectra of the DNA on the silver nanostructured silver substrate by e-beam lithography. Conditions: 8 mW power, 120 s, and 2-μm pitch.

parameters describing these arrays are discussed in this Section. Two different Raman spectra taken with the Renishaw μRaman apparatus with an Ar^+-ion laser (514.5 nm wavelength) at a power level of 8 mW are presented in Figs. 6 and 7. The Raman signatures are obtained on these substrates at edges of the silver nanodots and Figs. 6 and 7 report the Raman signatures obtained with 5- and 2-μm pitch, respectively.

D. MBs for the Detection of BRCA1 Gene

MBs are single strands of DNA, which are used as hybridization probes that can potentially detect SNPs [3], [19]. DNA-based MBs have been designed for the detection of the *BRCA1* gene, which is over expressed in breast cancer cells. The *BRCA1* is a human gene whose mutations have been associated with the increased probability of the occurrence of the breast cancer, as well as other types of cancers. These DNA-based MBs have been used to detect a sequence of DNA that occurs in the *BRCA1* gene.

MBs simultaneously form a stem-loop structure in solution thus bringing the fluorophore in close contact with the quencher. This causes the fluorescence of the quantum dots to be quenched due to the energy transfer process that could be described as a fluorescence resonance energy transfer [20] or nanoparticle surface energy transfer [21]. Such beacons are designed with quantum-dot fluorophores [22], [23] with emission at 605 nm (EBioscience) and monomaleimido gold nanoparticles of 1.4 nm diameter (Nanoprobes, Inc.) have been used as quenchers [24]. The beacons open out of this conformational state in the presence of the complementary strand, and the distance of the fluorophore from the quencher increases. As a result, the fluorescence intensity is higher leading to the specific detection of a DNA strand. We have also introduced a modification of the MB structure by adding six thymine residues on the 3′ terminal. The presence of the thymine chain reduces the steric hindrance, which can improve the performance of such hybridization probes [25].

The sequence used in the MB is 5′-NH_2C_6-CCTAGC **CCC TAT GTA TGC TCT TTG TTG TG** GCTAGG **TTTTTT**-C_3-S-S-3′. The stem is formed by the CCTAGC and GCTAGG sequences near the two ends of the DNA sequence, the **TTTTTT** strand of thymines is used as a spacer, and the amine group has a C6 spacer on the 5′ end. These MBs have been designed with protected thiol groups on their 3′ termini for binding to the gold nanoparticles and amine groups on the 5′ end for attachment to quantum dots. The complementary strand to be detected is: 5′-CTTAA **CAC AAC AAA GAG CAT ACA TAG GG** TTTCT-**3′**. The DNA strands were obtained from Integrated DNA Technologies (IDT).

The disulfide group on the 3′ terminal is reduced to a sulfhydryl group in the presence of a reducing agent, such as TCEP·HCl. The reduction takes place at room temperature for 30 min. 5–10 mM of TCEP is used for the reduction of 500-nM solutions of the MBs. Following the reduction, the gold nanoparticles are added at 1 μM concentration in sodium phosphate buffer with 1-μM EDTA salt and the reaction occurs at 4 $^\circ$C overnight. After this conjugation, a Millipore centrifugal filter is used to remove the nonconjugated gold nanoparticles. The quantum dots are then attached to the MB–gold nanoparticle conjugate at the 5′ end using the standard procedures mentioned in the previous section at lower concentration so that the ratios of the MB–gold nanoparticle conjugates to quantum dot is higher. These beacons are introduced in a concentration of 0.5 μM into a 5-mM solution of the complementary strand and photoluminescence (PL) spectra are acquired upon excitation with a HeCd laser. The representative spectra of Fig. 8 shows the comparison between the quenched and unquenched sample studied by the use of the 441 nm laser and reveal an on/off ratio of about 5:1.

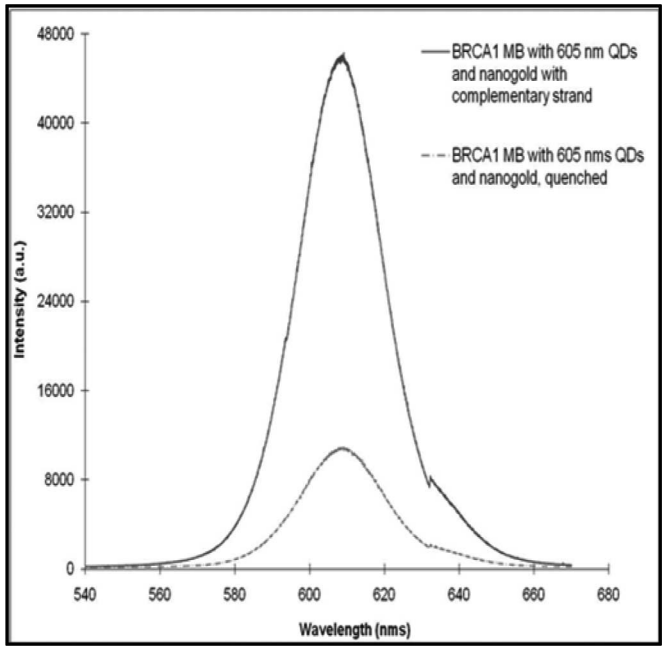

Fig. 8. PL measurement of the BRCA1 beacon in folded state and in the presence of the complementary strand. Conditions: 441-nm laser and 3 s.

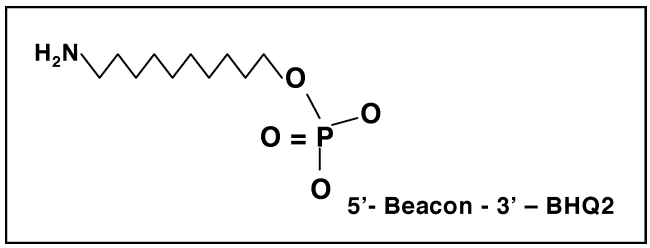

Fig. 9. Beacon sequence is modified with an amide group with 12 carbons on the 5′ terminal of the sequence. The 3′ terminal is modified with a BHQ2.

E. MBs for the In Vitro Food-Borne Pathogen Detection

In this section, beacons were designed and evaluated for the detection of the food-borne pathogen, *S. typhimurium* DT104. Conformational change in the antisense beacon was observed by monitoring the fluorescence of the quantum dot, which is distance-dependent in the fluorescence-resonant energy transfer between the quantum dot and its quencher. MBs have been successfully used in detecting the presence of Food-borne pathogens *in vitro*, such as through the use of quantitative PCR.

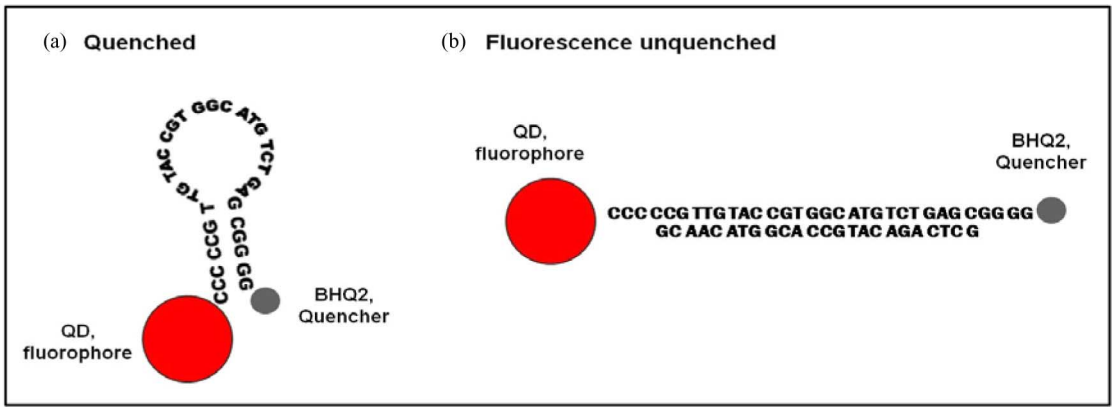

Fig. 10. Representation of the Beacon sequence modified with a BHQ2 at the 3′ end, and the 5′ end is attached to the quantum dots. (a) Folded state. (b) In presence of complementary strand.

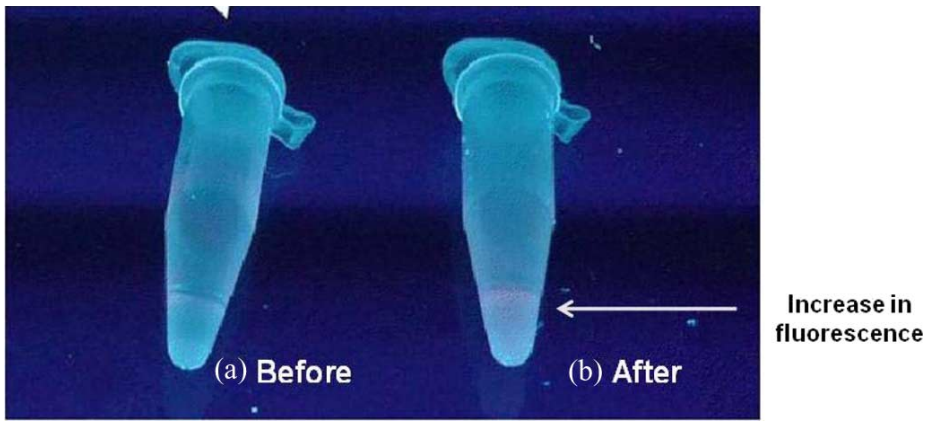

Fig. 11. (a) 10-nM beacon in 100-μL solution. Fluorescence emission from the quantum dots is quenched by BHQ2 before target DNA was added. (b) After 1 μL of target DNA was added, the total volume increases, but intensity of emission from the 605-nm quantum dots becomes stronger.

However, *in vivo* monitoring has only been demonstrated in mammalian cells [26], not for detecting pathogens in foods or transgenes in intact plants. Assays utilizing quantum dots have been used to detect *Escherichia coli* O157:H7 [27], *Cryptosporidium parvum* [28], and for the simultaneous detection of *E. coli* O157:H7 and *S. typhimurium* [29].

The food-borne pathogen in this study is *S. typhimurium*, DT104, a multidrug-resistant strain found in humans and animals. Most frequently, foods of animal origin, beef, poultry, milk, and eggs, are contaminated with *Salmonella* with the most recent outbreaks of salmonellosis for 2009, including peanut butter, pistachios, and alfalfa sprouts. Stock culture of *S. typhimurium* DT104 strain 2576 was obtained from the Department of Food Science and technology, University of Tennessee, Knoxville. Culture was grown overnight at 35 °C, 150 r/min in trypticase soy broth (TSB; Difco, Sparks, MD), and DNA was extracted using a GenElute Bacteria Genomic DNA kit.

Antisense beacon sequence (CCC CCG TTG TAC CGT GGC ATG TCT GAG CGG GG) was obtained from IDT, and was designed to detect a sequence (GCT CAG ACA TGC CAC GGT ACA ACG) specific to the *invA* gene from *Salmonella*.

The beacon DNA are modified with an amide group and with 12 extra carbon atoms on the 5′ terminal to provide a spacer for the relatively large quantum dot to bind to the DNA sequences so that they can bind to the carboxyl functioned quantum dot using 1-ethyl-3-[3-dimethylaminopropyl]carbodiimide hydrochloride (EDC or EDAC) cross-linkers (see Fig. 9).

Quantum dots in this study were obtained from EBioscience. This 10-μM quantum dot solution has optical excitation wavelengths in the wavelength range of 350–500 nm and a strong emission line at 605 nm. The surfaces of the quantum dots are modified with carboxyl groups so that quantum dots may bind to molecules with amide groups using cross-linkers. Black Hole Quencher2 (BHQ2; Biosearch Technologies, Inc.) is used to quench the quantum dots. BHQ2 quenchers were attached to the 3′ end of the sequence. These BHQ2 quenchers are capable of quenching fluorescence wavelengths in the range from 550 to 650 nm when the donor is within 10 nm of the quantum dot. The conformation of the beacon in its folded state and in the presence of a complementary strand is shown in Fig. 10. The "*mfold*" program is used to obtain conformational shape as well as the lowest free-energy state at room temperature [30]. BHQ2 was obtained from IDT along with the beacon sequence.

The beacons were synthesized using a procedure to optimize their switching capabilities. 200 pM of beacon sequences in 20-μL TE buffer was used to bind with 10-pM quantum dots using

600-nM EDC. Extra beacon sequences were used in order to decrease the amount of quantum dots binding to less than one beacon sequence. The beacon concentration is expected to be 0.37 μM in 27 μL. The beacon solution is centrifuged at a speed of 5000 $\times$ g, at 4 °C for 10 min, with a 50-k membrane. After filtering out the salt and the extra beacon sequences, the beacons were washed out with 1000-μL TE buffer. The beacon concentration resulting from this procedure is expected to be 10 nM.

To detect the DNA target sequence, a 100-μL beacon solution is used for *in vitro* tests. 100 pM of target DNA in 1-μL TE buffer was added to the 10-nM, 100-μL beacon solution and emitted more intense fluorescence compared with beacon solution without the target DNA (see Fig. 11).

The difference in fluorescence can be observed with the naked eye. Genomic DNA from *S. typhimurium* DT104 was detected *in vitro* using these probes with a fluorescence increase of 44% in the presence of target (fluorescence intensity of 921 in the control versus 1650 in the presence of target).

III. Conclusion

The vibrational modes of the selected DNA molecules have been studied under various conditions; these include the DNA self-assembled on silver-based substrates. The DNA modes include B- and Z-conformations, and DNA with functional groups that cause cleaving. The surface-enhanced Raman modes for each of these cases have been reported herein. These results indicated that environmental and conformation states lead to the shifts in the Raman-mode frequencies that provide a means of facilitating DNA identification. In this early study of SERS spectra, we have not attempted to determine how each functional component of our self-assembled DNA structures may have contributed to the full SERS spectra; future studies could usefully attempt to make such spectral assignments. This paper has also demonstrated the use of DNA MBs in detecting segments of the *BRCA1* gene and *Salmonella*. The procedures for optimizing the on–off fluorescence ratios for these MBs are discussed.

References

[1] X. Zhang, C. R. Yonzon, and R. P. Van Duyne, "Nanosphere lithography fabricated plasmonic materials and their applications," *J. Mater. Res.*, vol. 21, no. 5, pp. 1083–1092, 2006.

[2] M. Sackmann, S. Bom, T. Balster, and A. Materny, "Nanostructured gold surfaces as reproducible substrates for surface- enhanced Raman spectroscopy," *J. Raman Spec.*, vol. 38, pp. 277–282, 2007.

[3] S. Tyagi and F R. Kramer, "Molecular beacons: Probes that fluoresce upon hybridization," *Nat. Biotechnol.*, vol. 14, no. 3, pp. 303–308, 1996.

[4] Wolfram Saenger, *Principles of Nucleic Acid Structure*. New York: Springer-Verlag, 1984.

[5] S. C. Ha, K. Lowenhaupt, A. Rich, Y. Kim, and K. Kim, "Crystal structure of a junction between B-DNA and Z-DNA reveals two extruded bases," *Nature*, vol. 437, pp. 1183–1186, 2005.

[6] L. Rastislav, M. H. Tonya, J. T. Michael, and K. S. Sushil, "Using self-assembly to control the structure of DNA monolayers on gold: A neutron reflectivity study," *J. Amer. Chem. Soc.*, vol. 120, pp. 9787–9792, 1998.

[7] J. Malicka, I. Gryczynski, and J. R. Lakowicz, "Fluorescence spectral properties of labeled thiolated oligonucleotides bound to silver particles," *Biopolymers*, vol. 74, pp. 263–271, 2004.

[8] M. Guéron, J.-P. Demaret, and M. Filoche, "A unified theory of the B-Z transition of DNA in high and low concentrations of multivalent ions," *Biophys. J.*, vol. 78, no. 2, pp. 1070–1083, 2000.

[9] R. Levicky, T. M. Herne, M. J. Tarlov, and S. K. Satija, "Immobilization of nucleic acids at solid surfaces: Effect of oligonucleotide length on layer assembly," *Biophys. J.*, vol. 79, no. 2, pp. 975–981, 2002.

[10] C. Otto, T. J. J. Van Den Tweel, F. F. M. de Mul, and J. Greve, "Surface-enhanced Raman spectroscopy of DNA bases," *J. Raman Spec.*, vol. 17, no. 3, pp. 289–298, 1986.

[11] A. Barhoumi, D. Zhang, F. Tam, and N. J. Halas, "Surface-enhanced Raman spectroscopy of DNA," *J. Amer. Chem. Soc.*, vol. 130, no. 16, pp. 5523–5529, 2008.

[12] J. M. Benevides and G J. Thomas Jr., "Characterization of DNA structures by Raman spectroscopy: High-salt and low-salt forms of double helical poly (dG-dC in H_2O and D_2O solutions and application to B, Z and A-DNA*," *Nucleic Acids Res*, vol. 11, no. 16, pp. 5747–5761, 1983.

[13] M. Vasudev, T. Yamanaka, J. Yang, Y. Li, M. Dutta, and M. Stroscio, "Integrated DNA-nanoparticle complexes: synthesis—Electrical and optical properties," *ECS Trans.*, vol. 6, no. 15, pp. 53–55, 2007.

[14] H. Sugiyama and I. Saito, "Theoretical studies of GG-Specific photocleavage of DNA via electron transfer: Significant lowering of ionization potential and 5'localization of HOMO of stacked GG bases in B-form DNA," *J. Amer. Chem. Soc.*, vol. 118, pp. 7063–7068, 1996.

[15] T. Rajh, L. X. Chen, K. Lukas, T. Liu, M. C. Thurnauer, and D. M. Tiede, "Surface Restructuring of nanoparticles: An efficient route for ligand-metal oxide crosstalk," *J. Phys. Chem. B*, vol. 106, pp. 10543–10552, 2002.

[16] T. Paunesku, T. Rajh, G. Wiederrecht, J. Maser, S. Vogt, N. Stojicevic, M. Protic, B. Lai, J. Oryhon, M. Thurnauer, and G. Woloschak, "Biology of TiO_2–oligonucleotide nanocomposites," *Nat. Mater.*, vol. 3, pp. 343–346, 2003.

[17] A. Bykhovski, L. Xiaowei, T. Globus, T. Khromova, B. Gelmont, D. Woolard, A. C. Samuels, and J. O. Jensen, "THz absorption signature detection of genetic material of *E. coli* and *B. subtilis*," *Proc. SPIE*, vol. 5995, pp. 59950N.1–59950N.10, 2005.

[18] M. Vasudev, J. Yang, H. Jung, M. A. Stroscio, and M. Dutta, "Integrated nanostructure-semiconductor molecular complexes as tools for THz spectral studies of DNA," *IEEE Sensors J.*, vol. 10, no. 3, pp. 524–530, 2010.

[19] S. A. E Marras, F.R Kramer, and S. Tyagi, "Multiplex detection of single-nucleotide variations using molecular beacons," *Genet. Anal.*, vol. 14, pp. 151–156, 1999.

[20] P. R. Selvin, "The renaissance of fluorescence resonance energy transfer," *Nat. Struct. Biol.*, vol. 7, no. 9, pp. 730–734, 2000.

[21] E. Dulkeith, A. C. Morteani, T. Niedereichholz, T. A. Klar, and J. Feldmann, "Fluorescence quenching of Dye molecules near gold nanoparticles: Radiative and non-radiative effects," *Phys. Rev. Lett.*, vol. 89, no. 20, pp. 203002-1–203002-4, 2002.

[22] J. H. Kim, D. Morikis, and M. Ozkan, "Adaptation of inorganic quantum dots for stable molecular beacons," *Sens. Actuators B. Chem.*, vol. 102, pp. 315–319, 2004.

[23] N. C. Cady, A. D. Strickland, and C. A. Batt, "Optimized linkage and quenching strategies for quantum dot molecular beacons," *Mol. Cell. Probes*, vol. 21, pp. 116–124, 2007.

[24] B. Dubretet, M. Calame, and A. J. Libchaber, "Single-mismatch detection using gold-quenched fluorescent oligonucleotides," *Nat. Biotech.*, vol. 19, pp. 365–370, 2001.

[25] D. J. Maxwell, J. R. Taylor, and S. Nie, "Self assembled nanoparticle probes for recognition and detection of biomolecules," *J. Amer. Chem. Soc.*, vol. 124, pp. 9609–9612, 2002.

[26] D. P. Bratu, B. Cha, M. M. Mhlanga, F. R. Kramer, and S. Tyagi, "Visualization the distribution and transport of mRNAs in living cells," *Proc. Nat. Acad. Sci. USA*, vol. 100, no. 23, pp. 13308–13313, 2003.

[27] R. Edgar, M. McKinstry, J. Hwang, A. B. Oppenheim, R. A. Fekete, G. Giulian, C. Merril, K. Nagashima, and S. Adhya, "High-sensitivity bacterial detection using biotin-tagged phage and quantum-dot nanocomplexes," *Proc. Nat. Acad. Sci. USA*, vol. 103, no. 13, pp. 4841–4845, 2006.

[28] L. Y. Lee, S. L. Ong, J. Y. Hu, W. J. Ng, Y. Feng, X. Tan, and S. W. Wong, "Use of semiconductor quantum dots for photostable immunofluorescence labeling of Cryptosporidium parvum," *Appl. Environ. Microbiol.*, vol. 70, no. 10, pp. 5732–5736, 2004.

[29] L. Yang and Y. Li, "Simultaneous detection of *Escherichia coli* O157:H7 and Salmonella Typhimurium using quantum dots as fluorescence labels," *Analyst*, vol. 131, no. 3, pp. 394–401, 2006.

[30] M. Zuker, D. H. Mathews, and D. H. Turner, *Algorithms and thermodynamics for RNA secondary structure prediction: A practical guide in RNA biochemistry and biotechnology* (NATO ASI Series), J. Barciszewski and B. F. C. Clark, Eds., Norwell, MA, 1999.

Authors' photographs and biographies not available at the time of publication.